Molecular and Cellular Pathobiology

Cancer Research

SOX10 Ablation Arrests Cell Cycle, Induces Senescence, and Suppresses Melanomagenesis

Julia C. Cronin[1], Dawn E. Watkins-Chow[1], Art Incao[1], Joanne H. Hasskamp[2], Nicola Schönewolf[3], Lauren G. Aoude[4], Nicholas K. Hayward[4], Boris C. Bastian[5], Reinhard Dummer[3], Stacie K. Loftus[1], and William J. Pavan[1]

Abstract

The transcription factor SOX10 is essential for survival and proper differentiation of neural crest cell lineages, where it plays an important role in the generation and maintenance of melanocytes. SOX10 is also highly expressed in melanoma tumors, but a role in disease progression has not been established. Here, we report that melanoma tumor cell lines require wild-type SOX10 expression for proliferation and SOX10 haploinsufficiency reduces melanoma initiation in the metabotropic glutamate receptor 1 (*Grm1*^{Tg}) transgenic mouse model. Stable SOX10 knockdown in human melanoma cells arrested cell growth, altered cellular morphology, and induced senescence. Melanoma cells with stable loss of SOX10 were arrested in the G_1 phase of the cell cycle, with reduced expression of the melanocyte determining factor microphthalmia-associated transcription factor, elevated expression of p21WAF1 and p27KIP2, hypophosphorylated RB, and reduced levels of its binding partner E2F1. As cell-cycle dysregulation is a core event in neoplastic transformation, the role for SOX10 in maintaining cell-cycle control in melanocytes suggests a rational new direction for targeted treatment or prevention of melanoma. *Cancer Res; 73(18); 5709–18. ©2013 AACR.*

Introduction

Melanocytes are melanin-producing cells of neural crest origin located in the dermis and epidermis of the skin, the eye, the inner ear, and mucosal membranes. During development, differentiating melanocytes migrate from the neural tube to these distinct anatomic locations, each with unique cellular environments and potential for UV exposure. Malignancy of melanocytes results in melanoma, an aggressive and often fatal cancer. Moreover, melanoma incidence is increasing worldwide; the American Cancer Society describes melanoma as a disease affecting a wide-range of ages and projects diagnosis of approximately 76,600 new cases in 2013 (1). Classification of melanoma subtypes incorporates anatomic melanocyte location, degree of sun exposure, and histopathology in addition to genetic categorization based upon mutations in the mitogen-activated protein kinase (MAPK) signaling pathway components BRAF, NRAS, KIT, GNA11, and GNAQ (2–5). While recent targeted therapies to mutant BRAF hold promise, the majority of treated individuals with melanoma ultimately exhibit chemoresistance (6). Given the heterogeneity exhibited in melanoma, not only between tumor subtypes, but also the molecular diversity within individual lesions (7), there is a paramount need to identify and functionally assess additional genes fundamental to the regulation of melanoma growth and metastasis.

Increasing correlations are being discovered between genes that regulate developmental processes and the genes and signaling pathways mediating tumor progression through proliferation, invasion, and metastasis. Specification, survival, and differentiation of neural crest-derived lineages including melanocytes is dependent on SOX10 [SRY (sex-determining region Y)-box 10], a member of the high mobility group (HMG) domain SOX family of transcription factors. The approximately 50 known heterozygous germline mutations in SOX10 have been linked to developmental neurocristopathies Waardenburg syndrome (types II and IV) and PCWH (peripheral demyelinating neuropathy, central dysmyelinating leukodystrophy, Waardenburg syndrome, and Hirschsprung disease; ref. 8). SOX10 regulates many targets during neural crest development, including microphthalmia-associated transcription factor (MITF), which is necessary for normal melanocyte development. The regulation of MITF by SOX10 has implications in melanomagenesis, as MITF mutations and amplifications have been identified in a subset of melanomas (9, 10). MITF activates genes involved in melanocyte survival, such as

Authors' Affiliations: [1]Genetic Disease Research Branch, National Human Genome Research Institute, Bethesda, Maryland; [2]Maryland Melanoma Center at Medstar Franklin Square Medical Center, Baltimore, Maryland; [3]Department of Dermatology, University Hospital of Zurich, Zurich, Switzerland; [4]Queensland Institute of Medical Research, Oncogenomics Laboratory, Brisbane, Australia; and [5]Helen Diller Family Comprehensive Cancer Center, UCSF, San Francisco, CA

Note: Supplementary data for this article are available at Cancer Research Online (http://cancerres.aacrjournals.org/).

Corresponding Author: Stacie K. Loftus, NIH/National Human Genome Research Institute, 49 Convent Drive, Room 4A51, Bethesda, MD 20892. Phone: 301-594-1752; Fax: 301-402-2170; E-mail: sloftus@mail.nih.gov

doi: 10.1158/0008-5472.CAN-12-4620

BCL2 (11) and plays a key role in cell cycle via regulation of cyclin-dependent kinase inhibitor 2A (INK4A or CDKN2A), cyclin-dependent kinase inhibitor 1B (p27 or CDKN1B), and p53 (TP53; refs. 12–14).

In this study, we evaluate the role of SOX10 in melanomagenesis. We examine the mutation spectrum of *SOX10* in primary and metastatic melanoma tumor samples from multiple histologic subtypes and discover a low frequency of mutations. We assess the effects of reduced SOX10 levels on melanoma growth and survival and we show a G_1 cell-cycle arrest results from a loss of SOX10. We also confirm SOX10 expression is fundamental for melanomagenesis *in vivo* by showing that a reduction in SOX10 expression reduces tumor formation in the $Grm1^{Tg}$ melanoma mouse model. Together, these results indicate reducing SOX10 levels has fateful consequences for melanoma formation and expansion, suggesting SOX10 is a promising target for melanoma treatment.

Materials and Methods

PCR, sequencing, and mutational analysis

Melanoma genomic DNA samples were provided by Dr. Nicola Schönewolf (University Hospital of Zurich, Zurich, Switzerland) and Dr. Boris Bastian (University of California, San Francisco, CA). Additional samples from Dr. Nicholas Hayward were sequenced at the Queensland Institute of Medical Research (Brisbane, Queensland, Australia). Cell lines were provided by Joanne Hasskamp (Maryland Melanoma Center at MedStar Franklin Square Medical Center, Baltimore, MD), and the University of Arizona Cancer Center (UACC; Tucson, AZ). Genomic DNA was isolated using DNeasy Blood & Tissue Kits (Qiagen). PCR and sequencing primers (Supplementary Table S1) were designed using NetPrimer (http://www.premierbiosoft.com/netprimer/index.html) and synthesized by Invitrogen. *SOX10*-coding regions were amplified with TaKaRa LA Taq DNA Polymerase (Takara Bio) and sequencing carried out using BigDye Terminator v3.1 (Applied Biosystems). Sequence data were analyzed with Sequencher 4.9 Software (Gene Codes Corporation).

Cell Culture, siRNA transfection, and generation of stable short hairpin RNA lines

UACC melanoma cell line isolations were described previously (15); 0002-ARM-032702 (0002-ARM, IRB protocol number 97-79), and 0380-MMU-071802 (0380-MMU) cell lines were generated from patients at the Maryland Melanoma Center following standard surgical consent (16). Cell lines were maintained at 37°C with 5% CO_2 in Dulbecco's Modified Eagle Medium (UACC 1022) or Iscove's Modified Dulbecco's Medium (0380-MMU and 0002-ARM) supplemented with 10% FBS and 2 mmol/L L-glutamine (Invitrogen). To generate stable short hairpin RNA (shRNA) cell lines, melanoma cells were infected with pLKO1 lentiviral shRNA supernatant produced in 293T packaging cell line as described previously (17). Infected cells were selected with dose of puromycin antibiotic and cultured for 3 to 6 days before knockdown screening and functional assays. For transient transfection of siRNA duplexes, cells were treated with siRNA-Lipofectamine 2000 reagent complexes for 72 hours before harvesting. RNAi 27mer duplexes targeting *SOX10* were synthesized by Integrated DNA Technologies. siRNA sequences used in this analysis were: SOX10si_1-5′ AGACAAAGAAUGAGGUUAUUGGCACAG-3′, SOX10si_2-5′-GGUGCAACAGUCAACCUCCUUCUCCUC-3′, and nonsilencing control–siGENOME nontargeting siRNA pool #2 (Thermo Scientific).

Immunoblotting

Protein gels and Western blots were conducted using standard protocols. Primary antibodies were: monoclonal SOX10 (R&D Systems #MAB2864), monoclonal α-Tubulin (Calbiochem #CP06), total RB and Phospho-RB Ser807/811 antibody Kit (Cell Signaling Technology #9969), polyclonal E2F1 (Cell Signaling Technology #3742), monoclonal p16 (F-12 Santa Cruz Biotechnology #sc-1661), monoclonal p21 Waf1/Cip1 (Cell Signaling Technology #2946), monoclonal cyclin D1 (BD Pharmingen #G124–326), monoclonal p27 (Santa Cruz Biotechnology #sc-1641), polyclonal CDK2, CDK4, and CDK6 (Santa Cruz Biotechnology #sc-163, sc-601, and sc-177, respectively), and monoclonal MITF (generously provided by Heinz Arnheiter, NIH, Bethesda, MD). HRP-conjugated secondary antibody were from Jackson ImmunoResearch Laboratories.

Proliferation assay

Melanoma cell lines stably expressing nonsilencing or SOX10-specific shRNA were examined by seeding into 12-well plates (15,000 cells/well) and culturing for 14 to 16 days. Cells were fed fresh growth media once a week. Samples were analyzed every 48 to 72 hours by Vi-CELL counter (Beckman Coulter). All samples were run in duplicate, in two or three independent assays.

Immunohistochemistry

Cells were seeded into 8-well chamber CC2-coated slides (Thermo Fisher Scientific) one day before staining. Cells were rinsed with 1× PBS, fixed in 4% paraformaldehyde for 10 minutes, rinsed briefly with 1× PBS 0.1% Tween, then permeabilized with 0.1% Triton for 10 minutes. Following a 30-minute block in 1mg/mL bovine serum albumin (Sigma #A3059), cells were incubated 2 hours with primary antibodies in block (anti-SOX10, Santa Cruz, sc-17342; anti-HP1β, Millipore, MAB3448). Cells were then rinsed and incubated for 20 minutes in Alexa 488 or 568 secondary antibodies (Invitrogen) diluted in block. Cells were rinsed before mounting with ProLong Gold mounting media with DAPI (Invitrogen). Cell images were taken on Zeiss AxioImager.D2 upright microscope with AxioVision 4.8 software (Carl Zeiss Microscopy).

Senescence-associated β-galactosidase staining

Cultured cells were plated into 6-well dishes one day before staining. Cells were fixed and stained as per the manufacturer's protocol (Senescence β-Galactosidase Staining Kit, Cell Signaling Technology #9860). Stained cells were imaged with a Zeiss Axio Observer inverted scope with differential interference contrast brightfield microscopy. Ten random images were collected and cells counted with ImageJ 1.45s software.

Staining was conducted one week after infection or 72 hours after transfection in triplicate.

Fluorescence-activated cell sorting

Cultured cells were harvested by trypsinization, counted, and 5×10^5 cells were pelleted by centrifugation (1,000 rpm, 5 minutes). Cell pellets were resuspended in 500 μL propidium iodide and then incubated for 20 minutes at 37°C (NuCycl protocol; Exalpha Biologicals). Propidium iodide-stained cells were filtered and sorted on a FACS Calibur with 488 nm excitation (BD Biosciences).

Quantitative real-time PCR

Quantitative real-time PCR (qRT-PCR) was conducted on ABI 7500 (Applied Biosystems). RNA was isolated with RNeasy Mini Kits (Qiagen), three independent isolations were conducted for each sample. cDNA was generated with a Super Script III Kit (Invitrogen) as per the manufacturer's protocol. TaqMan gene expression assays (Applied Biosystems) for *SOX10* (Hs00366918_m1), *MITF* (Hs00165156_m1), *RB1* (Hs01078066_m1), *p27* (Hs01597588), and *E2F1* (Hs00153451_m1) were used with *GAPDH* (Hs02758991_g1) as reference gene. Alternatively, gene expression was measured with SYBR Green I PCR mix [15.2 μL diethyl pyrocarbonate (DEPC) water, 2.5 μL 10 × PCR buffer (10), 2.5 μL 10 mmol/L dNTP, 1.5 μL dimethylsulfoxide, 0.5 μL SYBR Green I diluted 1:1,000 in DEPC water, 0.5 μL of 50 μmol/L forward and reverse primers, and 25 μL TaKaRa LA Taq DNA polymerase) for p21 (*CDKN1A*). Cycling conditions were: 94°C, 2 minutes; 40 cycles at 94°C, 10 seconds; 60°C, 30 seconds; and 70°C, 30 seconds. Standard curve analysis was conducted on each gene (ABI 7500 Fast System v1.4.0 Software) in triplicate for each biologic sample. Primer sequences used in this analysis (5′ to 3′) were: p21 (*CDKN1A*) forward, ACTCTCAGGGTCGAAAACGG and reverse, CCTCGCGCTTCCAGGACTG (18); *GAPDH* forward, CATGACCACAGTCCATGCCATCACT and reverse, TGAGGTCCACCACCCTGTTGCTGTA (19).

Mouse husbandry and phenotype scoring

Mice were maintained in NIH animal facilities and all procedures approved by the Institutional Animal Care and Use Committee in accordance with NIH guidelines. *Grm1Tg (p18A4.B)1352Szc* mice, hereafter *Grm1*^{Tg} (20), were originally obtained on a mixed genetic background, then outcrossed repeatedly (>10 generations) to establish a colony on a predominantly C57Bl/6J background. Colonies of *Sox10tm1Weg* (hereafter *Sox10*^{LacZ}; ref. 21), *Mitf*$^{mi\text{-}vga9}$ (hereafter *Mitf*^{vga9}; ref. 22), and *Kit*^{tm1Alf} mice (hereafter *Kit*^{LacZ}; ref. 23) were also each maintained by repeated outcrossing to C57Bl/6J. Heterozygote carriers from each of the colonies were intercrossed with *Grm1*$^{Tg/+}$ heterozygotes and double heterozygote mice were backcrossed to *Grm1*$^{Tg/+}$ heterozygotes to generate mice for analysis.

To quantitate the severity of melanoma progression in *Grm1*^{Tg} mice, detailed observation and photodocumentation was used to assign numerical scores of 0 to 4 to the ears for two independent criteria, pigmentation and raised tumor severity. For scoring pigmentation, 0 indicated no visible pigmented nevi on the ear and 4 indicated that 90% to 100% of the ear was covered in continuous pigmentation. For scoring degree to which nevi were raised, 0 indicated that any visible pigmentation was flat with no detectable increased thickness of the skin and 4 indicated a significant raised tumor that was becoming necrotic and warranted euthanasia. Ventral spotting was also scored using a scale of 0 to 4 (0 = no ventral spotting; 4 = severe ventral spotting extending dorsally) as previously described (24).

Results

Assessment of somatic SOX10 mutations across melanoma subtypes

Melanoma can arise in different histologic locations, resulting in numerous subtypes with distinct protein expression patterns and genomic aberrations (25). Previously, we identified intragenic mutations in the *SOX10* locus in a subset of samples from both primary and metastatic melanoma (10). To fully evaluate the contribution of *SOX10* mutations to melanoma progression, we expanded our analysis of *SOX10* coding variations with an additional 153 melanoma samples representing various histologic subtypes (Table 1). Only one novel *SOX10* alteration was observed: a G to T substitution encoding a nonsynonymous amino acid change (p.P217L) in a cell line derived from an acral lentiginous melanoma tumor. This altered proline is 3′ of the HMG binding domain and is evolutionarily conserved from mammals to chicken. Although we were unable to validate that this coding alteration occurred somatically in this sample as normal genomic DNA from this

Table 1. Sequencing of SOX10 across various melanoma histologies

Institution	Sample number	Histology	SOX10 Mutations
University of Arizona Cancer Center	12	Superficial spreading/cutaneous	None
Maryland Melanoma Center at Medstar Franklin Square	14	Superficial spreading/cutaneous	None
American Type Culture Collection	1	Superficial spreading/cutaneous	None
Queensland Institute of Medical Research	41	Superficial spreading/cutaneous	None
University Hospital of Zurich (Zurich, Switzerland)	26	Mucosal, acral lentiginous	1/26 (3.8%)
University of California	59	Acral, mucosal, lentigo, desmoplastic	None
Total	153		1/153 (0.65%)

patient was unavailable, query of the dbSNP database indicated the predicted P217L variant has not been observed previously (National Center for Biotechnology Information, dbSNP short genetic variations, www.ncbi.nlm.nih.gov, accessed August 22, 2012), suggesting this *SOX10* DNA change is unique. Overall, these findings suggest that maintenance of SOX10 function is required for melanomagenesis, as melanoma cells favor the retention of a wild-type SOX10.

SOX10 knockdown in melanoma cells results in G_1 arrest and cell senescence

To assess whether SOX10 is required for melanoma cells *in vitro*, we conducted RNAi-mediated knockdown. Three melanoma cell lines were transduced with 2 different SOX10-specific lentiviral RNAi hairpins (shSOX10) and compared with lines transduced with a nonsilencing control hairpin. One week after infection, the shSOX10 lines showed reduced SOX10 protein levels and the cells became enlarged, flat, and translucent (Fig. 1A and B). These cells also showed arrested or slowed growth (Fig. 1C). Analysis of five additional melanoma lines showed consistent results, with 6 of the 8 lines displaying altered cellular morphology and slowed growth resulting from SOX10 knockdown (data not shown). Three of these 6 lines were selected for further functional analysis: the 0002-ARM and UACC 1022 cell lines, which contain V600E and L597S BRAF mutations, respectively, and the 0380-MMU cell line, which harbors an NRAS Q61K mutation.

To further characterize the arrested growth we observed in the shSOX10 lines, we stained for β-galactosidase (SA-β-Gal), a biomarker of cellular senescence (Fig. 1D). Significant increases in SA-β-Gal activity were seen in all 3 lines when stably transduced with shSOX10 hairpins (Fig. 1E), suggesting that loss of SOX10 induces senescence in melanoma cells. Another hallmark of cellular senescence, senescence-associated heterochromatin foci (SAHF), was observed upon chromatin binding protein HP1β immunostaining (Fig. 1F and

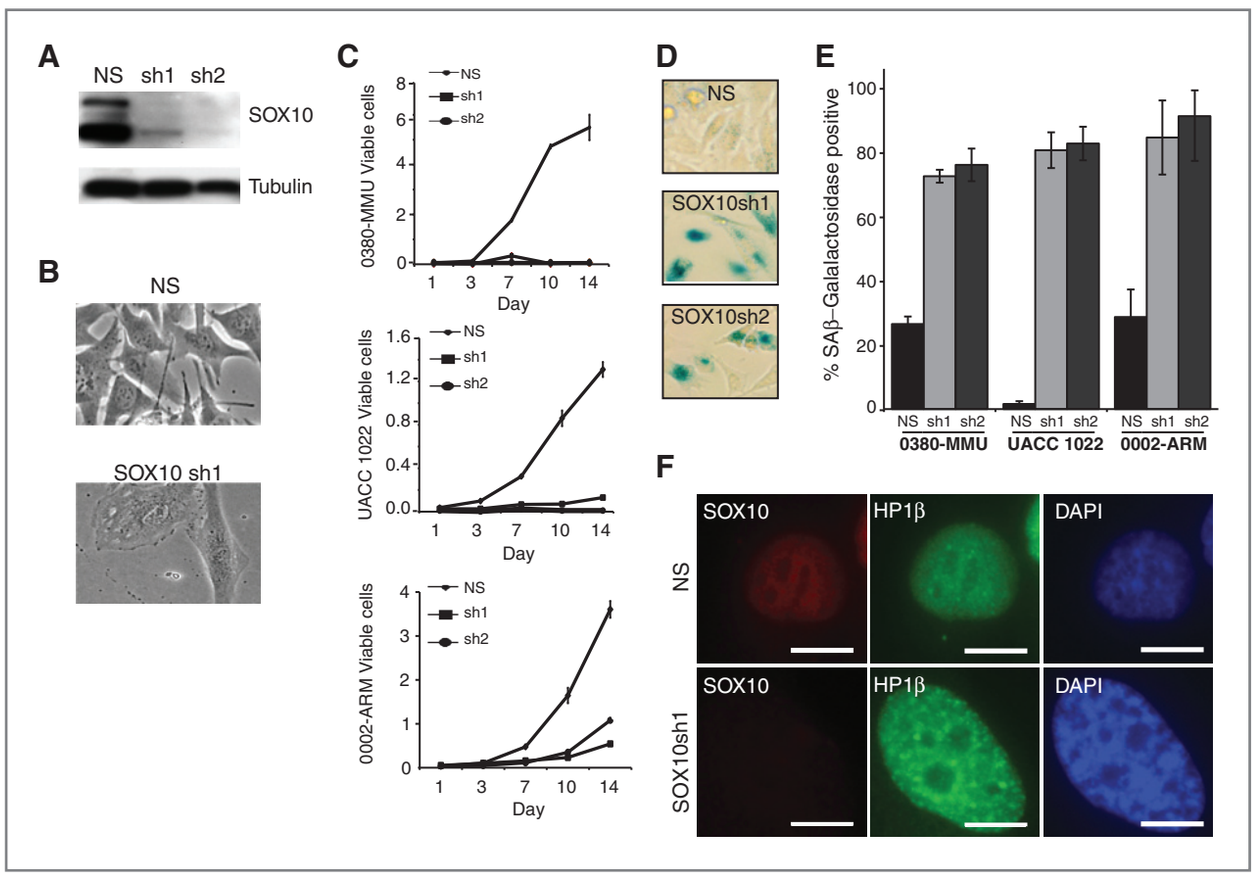

Figure 1. SOX10 depletion triggers arrested growth and melanoma cell senescence. A, Western blot analysis of SOX10 expression in 0380-MMU cell lysates stably transduced with a nonsilencing control hairpin (NS) or SOX10-specific lentiviral RNAi hairpins (sh1 and sh2). B, phase-contrast images of 0380-MMU stable cell lines, one week after infection with nonsilencing control hairpin or SOX10sh1. C, proliferation assays for 0380-MMU, UACC 1022, and 0002-ARM cell lines transduced with nonsilencing control hairpin, sh1, or sh2. Cells were counted in triplicate 1 to 14 days after plating and proliferation assays were conducted at least twice with subsequent infections. D, representative images of 0380-MMU cells stained for SA-β-Gal activity one week after infection with nonsilencing control hairpin, SOX10sh1, and SOX10sh2. E, significant increases in the percentage of SA-β-Gal–positive cells were seen in SOX10sh lines relative to nonsilencing control hairpin lines as determined by Student *t* test (for 0380-MMU, sh1 $P < 7.32 \times 10^{-5}$, sh2 $P < 7.95 \times 10^{-3}$; for UACC 1022, sh1 $P < 5.49 \times 10^{-11}$, sh2 $P < 2.17 \times 10^{-8}$; and for 0002-ARM, sh1 $P < 2.90 \times 10^{-5}$, sh2 $P < 8.80 \times 10^{-5}$). F, stably transduced UACC 1022 cell lines stained with anti-SOX10, anti-HP1β antibodies, and DAPI nuclei counterstain. HP1β staining indicated the presence of SAHF in SOX10sh1 cells. Scale bar, 10 μm.

Supplementary Fig. S1). Upon loss of SOX10 protein, the cells showed more severe punctate staining of HP1β as a result of chromatin rearrangements brought on by senescent fate.

The shSOX10 cells showed no increase in APC-Annexin V staining as compared with controls, indicating no increase in apoptosis (data not shown). Quantitation of the number of cells in each phase of the cell cycle by fluorescence-activated cell sorting (FACS) analysis showed that SOX10 knockdown cells consistently showed a significant increase in the population of cells in G_1 phase (Fig. 2A), indicative of G_1 arrest and decreased cell-cycle progression. Taken together, these data suggest SOX10 is required for proliferation of melanoma cells.

SOX10 knockdown results in reduced E2F1 and RB levels

The RB–E2F1 complex gates a fundamental checkpoint regulating progression through the G_1 phase of the cell cycle (7). Phosphorylation releases RB from E2F1 during G_1 and is required for the accumulation of transcriptionally active E2F1 (26). Thus we evaluated E2F1 and RB protein levels by Western blot in SOX10 knockdown cells. In all three melanoma lines, SOX10 knockdown led to reduced levels of E2F1 protein and total RB protein (Fig. 2B). Consistent with these results, we found *E2F1* transcript levels decreased upon SOX10 knockdown (Fig. 2C), however, no change in *RB* mRNA levels were seen (Fig. 2C) despite seeing less RB protein. When the degree of RB phosphorylation was evaluated with an antibody specific for RB serine residues Ser807 and Ser811, we observed a decrease in levels of phosphorylated RB (Fig. 2B). These data suggest that the total RB protein level decreases as a result of a loss of stable phosphorylated RB and are consistent with the G_1 arrest observed. A similar destabilization of RB protein leading to G_1 arrest has been reported in PAX8 knockdown experiments (27).

shSOX10-induced G_1 arrest is not mediated by p53 signaling

The p53 pathway regulates the G_1 cell-cycle checkpoint, and p53 activation has been shown to result in melanoma cell-cycle arrest (28). Therefore we measured p53 protein levels in SOX10 knockdown cells. In the 0002-ARM cell line, p53 levels decreased with reduced SOX10 expression, however no change in p53 levels was observed in 0380-MMU cells (Fig. 2B). For the UACC 1022 line, p53 was undetectable in both the control cells and shSOX10 lines (Fig. 2B). Sequencing of the *TP53* locus in the UACC 1022 line identified a premature stop codon along with loss of heterozygosity (R195X; data not shown), indicating UACC 1022 is null for p53 protein signaling. As growth arrest was observed in all three lines, independent of p53 status, the G_1 arrest observed in shSOX10 cells is not solely mediated through the p53 signaling pathway.

SOX10 knockdown results in decreased MITF and increased CDK inhibitors p21 and p27

As knockdown of MITF in melanoma cell lines has been shown to produce a similar decrease in growth rate and G_1 cell-cycle arrest (29) and *MITF* is a well established downstream transcriptional target of SOX10 (30), we assessed MITF expression upon shSOX10 knockdown. Reduced MITF protein was

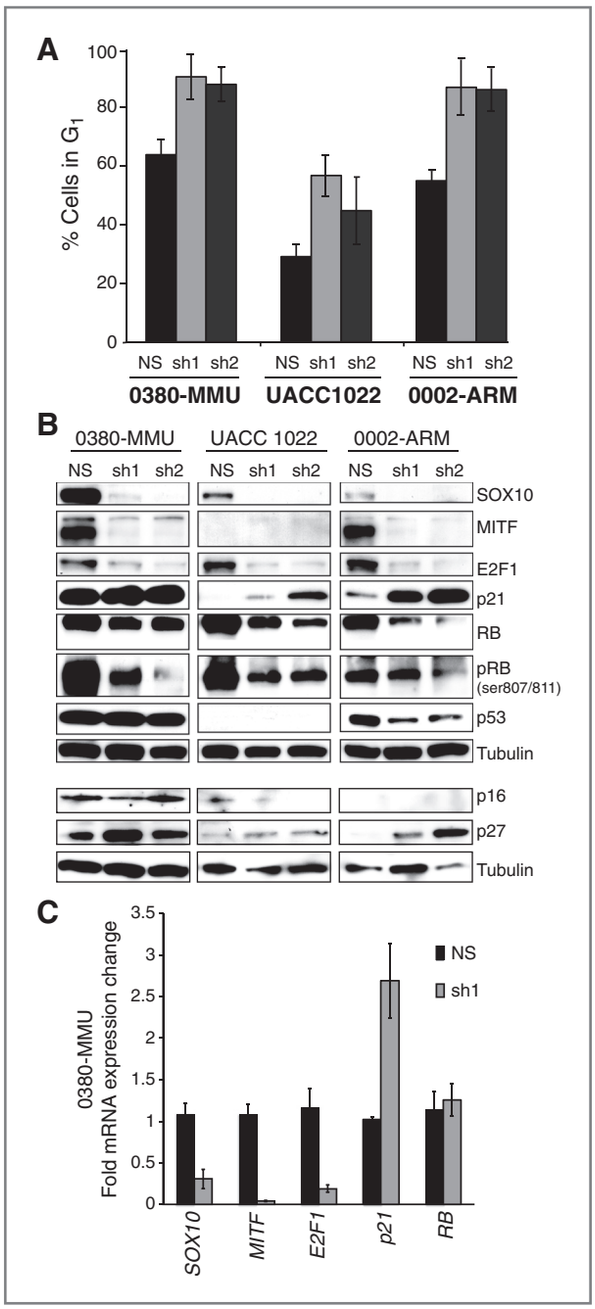

Figure 2. Cell-cycle arrest and expression changes in cell-cycle regulators are observed upon stable loss of SOX10. A, significant increases in G_1 cell populations were observed in 0380-MMU, UACC 1022, and 0002-ARM lines stably transduced with SOX10-specific hairpins (sh1 and sh2) relative to lines stably transduced with a nonsilencing control hairpin (NS; Student *t* test *P* values were 0380-MMU, sh1 = $P < 0.007$, sh2 = $P < 0.026$; UACC 1022 sh1 = $P < 0.026$, sh2 = 0.17; 0002-ARM sh1 = $P < 0.023$, sh2 = $P < 0.03$). FACS analysis on each line was repeated twice with subsequent infections. B, Western blot analysis of the effects of nonsilencing control hairpin, sh1, and sh2 stable transduction in each line on important cell-cycle regulatory proteins. C, qRT-PCR of RNA isolated from 0380-MMU nonsilencing control hairpin and sh1 stable lines showed significant changes in *SOX10* ($P < 0.006$), *MITF* ($P < 0.0005$), *E2F1* ($P < 0.005$), and *p21* ($P < 0.016$) expression as determined by Student *t* test. Data are fold change normalized to control and the average of three replicate assays.

observed upon shSOX10 knockdown in both 0380-MMU and 0002-ARM cells (Fig. 2B), whereas MITF protein expression was undetectable by Western blot analysis in UACC 1022 control cells (Fig. 2B).

Given these altered MITF expression levels, we looked for consistent alterations in G_1 cell-cycle regulators across the three lines. CDK2, itself a downstream target of MITF transactivation (31), decreased in both the 0380-MMU and UACC 1022 shSOX10 cells and increased in the 0002-ARM shSOX10 cells (Supplementary Fig. S2). However, no consistent change in total expression level for CDK4, CDK6, or cyclin D1 proteins was observed (Supplementary Fig. S2), thus CDK protein expression levels did not provide a unified mechanism to explain the loss of phosphorylated RB protein observed in shSOX10 cells.

We next evaluated protein levels of p16 (*CDKN2A*), p21 (*CDKN1A*), and p27 (*CDKN1B*) following SOX10 knockdown (Fig. 2B). Lowered MITF levels leading to G_1 arrest have been correlated with an increase in p27 levels (12) and with decreased levels of p21, as MITF directly regulates p21 transcription (32, 33). We observed moderate p16 expression in 0380-MMU cells; however, p16 levels remained unchanged following SOX10 knockdown. We consistently observed increases in p27 levels in all three cell lines as a result of SOX10 knockdown (Fig. 2B), similar to previous MITF knockdown studies (12). However, SOX10 knockdown caused an increase in p21 protein in all three-cell lines (Fig. 2B), thus showing a distinct difference from the MITF knockdown results.

Altered *MITF* and *p27* gene expression occur before G_1 arrest

To assess changes in transcript levels before G_1 arrest, we conducted a transient, 72-hour siRNA knockdown of SOX10. In both 0380-MMU and UACC 1022 cell lines, siSOX10 knockdown led to decreased SOX10 protein (Supplementary Fig. S3), however, siSOX10 knockdown did not increase SA β-gal activity or the G_1 cell population (Fig. 3A and B). Consistent with the stable shSOX10 knockdown results, we found transient siSOX10 treatment reduced *MITF* mRNA in both cell lines, increased *p27* mRNA in both cell lines, increased *p21* mRNA in 0380-MMU cells (but had no effect on *p21* in UACC1022 cells), and had no effect on *RB* mRNA levels in both lines (Fig. 3C and D). *E2F1* message changes seemed to be cell-type dependent (Fig. 3C and D).

Reduction of SOX10 expression *in vivo* suppresses melanomagenesis

To assess the role of SOX10 in melanoma progression *in vivo*, we used a mouse model of *Sox10* haploinsufficiency ($Sox10^{LacZ/+}$; ref. 21) crossed with a $Grm1^{Tg}$ mouse melanoma model (20). In human melanomas, glutamate receptor pathway activation is observed in tumors harboring recurrent mutations in the glutamate receptor genes *GRM3* (34) and *GRIN2A* (35). Similarly, $Grm1^{Tg}$ mice harbor a transgene insertion that causes overexpression of *Grm1*, activates the glutamatergic pathway and causes numerous, pigmented nevi at weaning in heterozygous and homozygous mice (Fig. 4A). Nevi in homozygotes ($Grm1^{Tg/Tg}$) are raised by 2 to 3 months of age and typically necessitate euthanasia by 5 months of age. We crossed $Grm1^{Tg/Tg}$ mice with $Sox10^{LacZ/+}$ mice, then double heterozygotes were backcrossed to $Grm1^{Tg/Tg}$ mice, thus generating $Grm1^{Tg/+}$ and $Grm1^{Tg/Tg}$ offspring that were also haploinsufficient for *Sox10* ($Grm1^{Tg/+}$;$Sox10^{LacZ/+}$ and $Grm1^{Tg/Tg}$;$Sox10^{LacZ/+}$, respectively) along with $Grm1^{Tg/+}$ and $Grm1^{Tg/Tg}$ littermates. The extent of pigmentation and severity of raised tumors visible on the ears of 3- to 5-month-old mice was quantitatively scored and compared among genotypes (Fig. 4A–C). *Sox10* haploinsufficiency significantly reduced the number of pigmented nevi in both $Grm1^{Tg/+}$ and $Grm1^{Tg/Tg}$ mice ($P < 0.005$), and also the severity of raised nevi in $Grm1^{Tg/Tg}$ mice ($P < 0.05$). An extended tumor latency was also observed, with raised tumors first appearing in $Grm1^{Tg/Tg}$;$Sox10^{LacZ/+}$ mice at 5 to 6 months versus 2 to 3 months in $Grm1^{Tg/Tg}$ mice (data not shown).

Interestingly, the $Grm1^{Tg}$ transgene did not suppress the hypopigmentation (belly spots) that is normally observed in $Sox10^{LacZ/+}$ mice due to a developmental reduction in melanoblast number (Fig. 4D and E). This indicates that $Grm1^{Tg}$ does not cause a developmental expansion of melanoblasts and suggests that the role of SOX10 in melanoma suppression is independent of its effect on embryonic melanoblast number. Another white spotting allele with a developmental reduction in melanoblasts, Kit^{LacZ}, was not sufficient to suppress melanoma in $Grm1^{Tg}$ (Supplementary Fig. S4), which is consistent with separate roles for SOX10 in developmental melanoblast number and melanoma formation in the $Grm1^{Tg}$ model.

To understand the role of *Mitf* in the $Sox10^{LacZ}$ suppression of $Grm1^{Tg}$ mouse melanoma lesions, $Grm1^{Tg/Tg}$ mice were crossed to mice that harbor a transgene disruption that results in a functionally null allele of *Mitf*. In contrast with the $Grm1^{Tg/+}$;$Sox10^{LacZ/+}$ and $Grm1^{Tg/Tg}$;$Sox10^{LacZ/+}$ mice, heterozygosity for the $Mitf^{vga9}$ allele did not suppress the development of hyperpigmented, raised lesions in the $Grm1^{Tg/+}$;$Mitf^{vga9/+}$ and $Grm1^{Tg/Tg}$;$Mitf^{vga9/+}$ mice (Supplementary Fig. S4). Of note, $Mitf^{vga9/vga9}$ homozygotes lack melanocytes and thus could not be analyzed (22, 36). In summary, *Sox10* haploinsufficiency is sufficient to suppress the phenotype of $Grm1^{Tg}$ mice, indicating an essential role of SOX10 in melanoma progression.

Discussion

Melanoma is an aggressive tumor type that progresses rapidly and exhibits resistance to most current therapeutic interventions. Although targeted therapies to known tumor suppressor and oncogenic players in melanoma cells may achieve responses, patients are subject to relapse (37, 38). This study focuses on the role of SOX10 in melanoma and supports mounting evidence suggesting SOX10 is an important lineage-specific target for patient intervention. Previous studies have detailed broad expression of SOX10 in melanoma tumor samples across various stages of disease, further suggesting a necessity for this protein in melanoma (39–42).

Our sequencing analysis reveals a low frequency of intragenic mutations in *SOX10*, suggesting a preference for wild-type SOX10 protein in melanoma formation and maintenance.

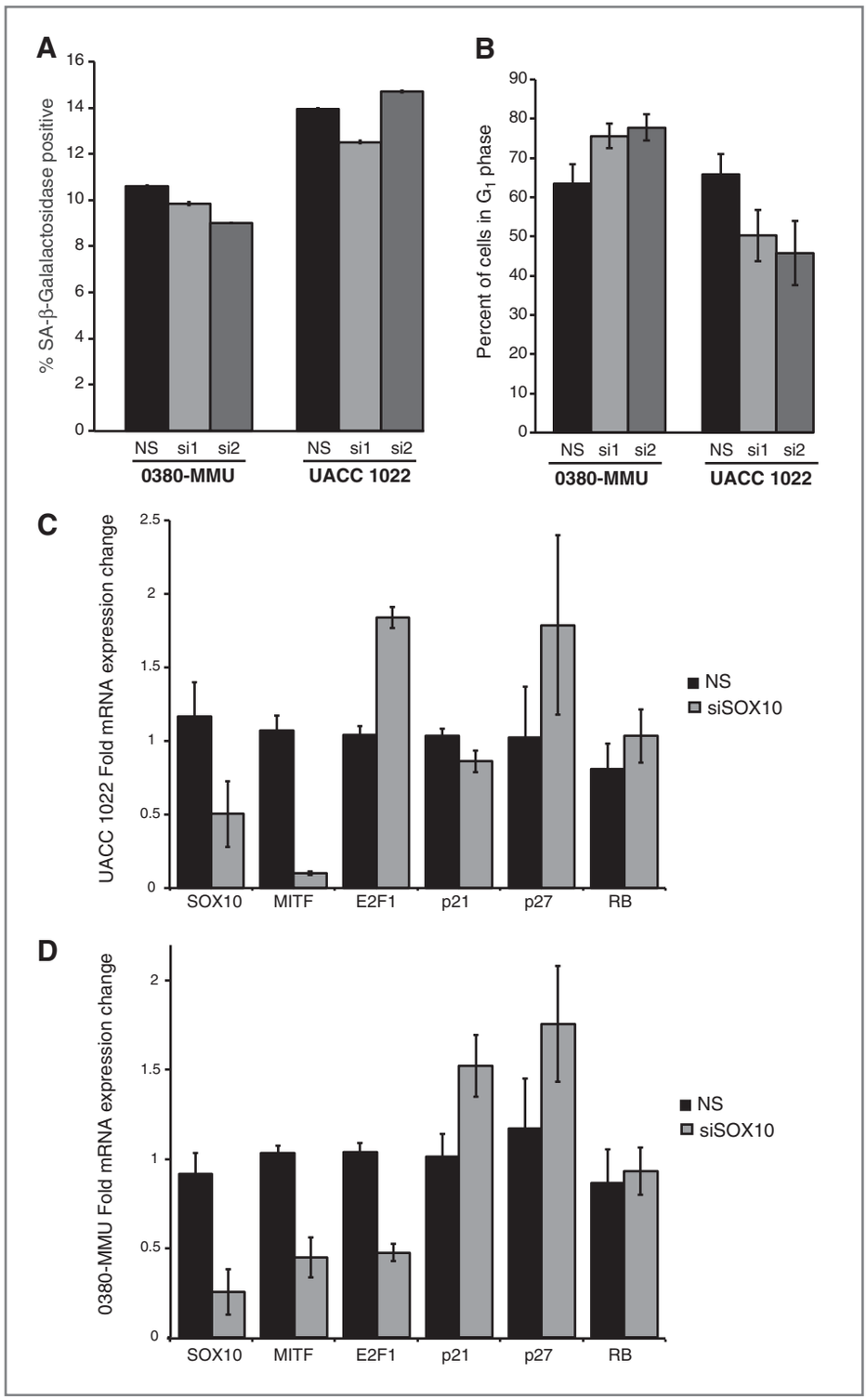

Figure 3. Altered MITF, p21, and E2F1 expression precedes G_1 cell-cycle arrest. A, quantification of the percentages of SA-β-Gal–positive cells in 0380-MMU and UACC 1022 cells transiently transfected with nonsilencing (NS) or SOX10-specific (si1 and si2) siRNA showed no significant differences. B, no significant differences were seen in G_1 cell populations in 0380-MMU and UACC 1022 melanoma cell lines transiently transfected with nonsilencing control hairpin, si1, or si2. FACS analysis on independent cell lines was repeated twice with subsequent transfections. C–D, qRT-PCR analysis of UACC 1022 (C) and 0380-MMU (D) cell lines transiently transfected with nonsilencing control hairpin or siSOX10. Data are fold change normalized to nonsilencing control. siSOX10-transfected UACC 1022 cells showed significant changes in expression of *SOX10* ($P < 0.05$), *MITF* ($P < 0.0004$), and *E2F1* ($P < 0.001$). siSOX10-transfected 0380-MMU cells showed significant changes in the expression of *SOX10* ($P < 0.01$), *MITF* ($P < 0.007$), and *E2F1* ($P < 0.001$); *p21* and *p27* showed increased expression that did not achieve statistical significance. Data analyzed by Student *t* test.

Recent research has shown the rate of "passenger" mutations, propagated by clonal expansion without any growth advantage, is higher in cutaneous melanoma than in solid tumors (43). This high passenger mutation rate was exemplified in genomic sequencing of 121 melanoma samples, where 518 genes were found to have mutations in more than 10% of melanoma samples (5). Previously, we identified nine *SOX10* mutations from 2 small, distinct melanoma patient cohorts.

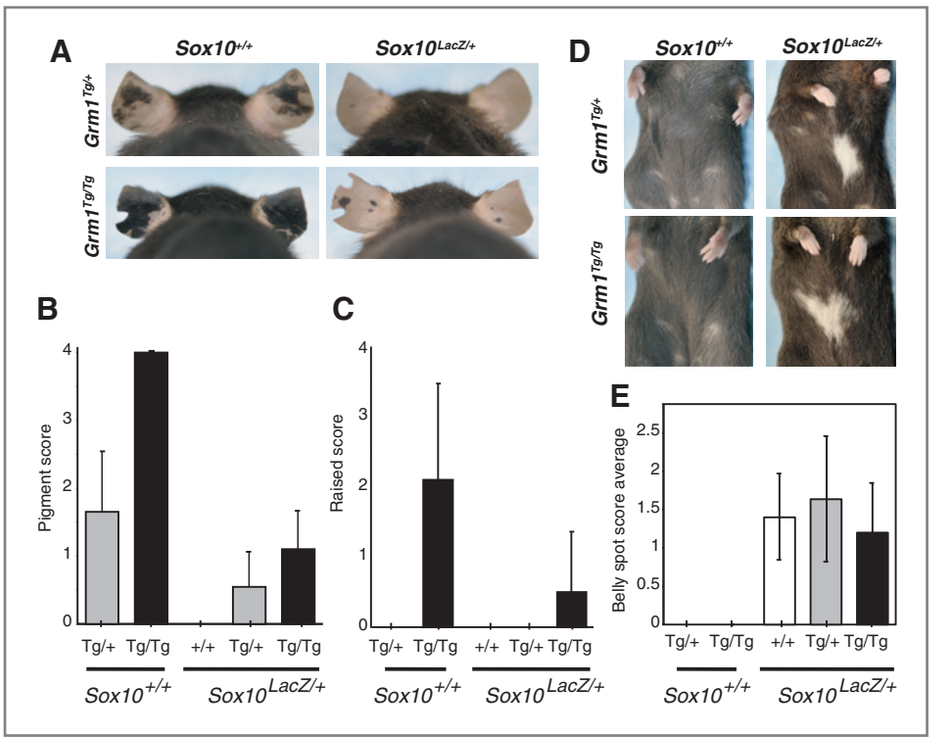

Figure 4. SOX10 expression is required for melanoma progression *in vivo*. A, $Grm1^{Tg/+}$;$Sox10^{+/+}$ mice show moderate ear hyperpigmentation (top left). This phenotype is exaggerated in $Grm1^{Tg/Tg}$;$Sox10^{+/+}$ mice, where the pigmented lesions are raised (bottom left). Haploinsufficiency for SOX10 ($Sox10^{LacZ/+}$) in conjunction with one or two $Grm1^{Tg}$ alleles reduces pigmented ear lesions (right two panels). B–C, $Grm1^{Tg}$ phenotypic severity either alone or in the context of *Sox10* haploinsufficiency was quantitatively measured by scoring each individual animal on a scale of 1 to 4 for the extent of pigmentation (B) and burden of raised tumors (C). *Sox10* haploinsufficiency significantly reduced pigmented nevi ($P < 0.005$) in both $Grm1^{Tg/+}$ and $Grm1^{Tg/Tg}$ mice and also the extent to which they were raised ($P < 0.05$) in $Grm1^{Tg/Tg}$ mice (Mann–Whitney test with Bonferonni correction). D, no ventral spotting was observed in $Grm1^{Tg/+}$ or $Grm1^{Tg/Tg}$ mice that were also $Sox10^{+/+}$ (left) and the presence of one or two $Grm1^{Tg/+}$ alleles did not affect ventral spotting caused by the $Sox10^{LacZ}$ allele (right; mice shown received a spotting severity score of 2). E, quantitative scoring of belly spots in $Sox10^{LacZ}$; $Grm1^{+/+}$, $Sox10^{LacZ}$; $Grm1^{Tg/+}$, and $Sox10^{LacZ}$; $Grm1^{Tg/Tg}$ mice showed no significant differences ($P = 0.3342$; Kruskal–Wallis nonparametric one-way ANOVA).

We identified 3 of 50 mutations in metastatic samples from individuals enrolled in a single clinical trial and 7 of 55 mutations from primary samples for a combined mutation rate of 8.5%. Of these, only the three mutations identified from samples obtained from the single metastatic cohort of patients were characterized by either an early truncation of SOX10 or an alteration leading to a C-terminal extension of SOX10 and were found to have reduced SOX10 functional activity (10). Given that the combined mutation rate (8.5%) falls within the range anticipated for melanoma and that all of the confirmed functional mutations were ascertained from one patient cohort, we felt further analysis of the *SOX10* locus was warranted.

In this analysis, we increased sample numbers of mucosal and lentiginous melanoma subtypes and increased the diversity of clinical sources from which samples were collected, to reduce the potential for ascertainment bias. From this diverse sample cohort we found only 1 of 153 (<1%) of melanoma samples mutated for SOX10. This rate is consistent with the SOX10 mutation rate identified from recent large scale sequencing of metastatic melanoma (5). These data show that the SOX10 mutation rate is less than the passenger mutation rate, suggesting the potential preference for wild-type SOX10 protein in melanoma formation and maintenance.

Consistent with this finding, we hypothesize that SOX10 regulates melanoma cell proliferation and cell-cycle regulation via multiple, convergent pathways regulating RB and E2F1 levels. Reduction in SOX10 levels results in increased expression of p21 and p27, inhibitors of CDKs, which regulate multiple, sequential phosphorylation events on RB necessary for cell-cycle progression. The E2F1–RB complex provides a cellular checkpoint for cell-cycle progression out of G_1. RB in its hypophosphorylated state prevents cells from entering S-phase and arrests them at G_1. E2F1 level regulation is a key mediator of progression through G_1, as E2F1 functions to activate downstream targets required for entry into S-phase. As we observed a change in E2F1 RNA levels combined with a senescent cellular phenotype when SOX10 expression was decreased in melanoma cell lines, we postulate that SOX10, or a downstream target, is required for proper regulation of *E2F1* and subsequent control of cell proliferation through RB–E2F1 signaling. This is in contrast with what is observed for RB, where RB protein is reduced but transcript expression is unchanged following SOX10 reduction. We cannot exclude the possibility that SOX10 could indirectly stabilize the RB protein to prevent proteasomal degradation. In fact, the reduction in total RB protein may be a result of SOX10-mediated reduction

in E2F1 levels, as reduced levels of active RB have been shown to be a direct consequence of decreased E2F1 expression (44) as well as increased p27 and p21 levels, ultimately resulting in more unstable hypophosphorylated RB protein (45).

Studies involving human melanoma cell lines can be limited because of the heterogeneity and phenotypic variations resulting from context-dependent effects on the genome. The melanoma cell lines described in this study mirror that heterogeneity, showing differences in p53 status, $p16^{ARF}$ and MITF expression levels, and mutation status of the major oncogenes *NRAS* and *BRAF*. Despite these notable variations, a dysregulated cell cycle with altered RB and E2F1 levels was consistently observed upon loss of SOX10 protein. Initially we hypothesized that MITF, which itself is a direct transcriptional target of SOX10, was appropriately poised to be the responsible transcription factor. Although RNAi-mediated reduction of MITF also leads to a senescent morphology and G_1 cell arrest (13), this occurred in conjunction with a decrease in p21 expression, which was not observed in our study of SOX10 knockdown. These results may have potential implications clinically given the heterogeneity that exists within melanoma tumors. Importantly, the consistent observation that SOX10 is required for proliferation of melanoma cells suggests that SOX10 or its downstream targets are involved in the regulation of cell cycle.

The frequent acquired resistance to current BRAF inhibitors observed in recent clinical trials is mediated by reacquisition of increased MAPK signaling (46). These results highlight the need for a more comprehensive understanding of all aspects of cell-cycle dysregulation that occurs as a result of increased MAPK signaling in tumors and the need to evaluate additional mechanisms that have the capacity to reduce cell proliferation and tumor formation. We find that SOX10 has a pivotal role in melanoma cell proliferation not only in cell culture, but also *in vivo*, as *Sox10* haploinsufficiency prevents the formation of hyperpigmented lesions observed in the $Grm1^{Tg}$ mouse melanoma model. A recent study by Shakhova and colleagues reported a similar reduction in tumor formation when SOX10 levels were reduced in the context of the $Nras^{Q61K}$-driven mouse melanoma model (47). Together, these studies show that distinct melanoma drivers require SOX10 for tumor formation and maintenance. Both NRAS and GRM1 activate the MAPK and PI3K/AKT signaling pathways, which are fundamental to melanomagenesis. Given that both the $Nras^{Q61K}$ and the $Grm1^{Tg}$ mouse melanoma models are rescued with *Sox10* haploinsufficiency, SOX10 may occupy an important position of regulation of oncogenic cell-cycle progression downstream of one or both of these signaling pathways. Interestingly, the $Grm1^{Tg}$ mouse melanoma model is not rescued with the $Mitf^{vga9}$ mouse, suggesting that either this cross did not result in a sufficient loss in *Mitf* expression, as $Mitf^{vga/+}$ mice have been shown to exhibit a 50% reduction in melanocyte MITF levels (22) or that SOX10 is involved in key melanoma pathways independent of its regulation of *Mitf* levels. When these data are combined with the extensive occurrence of SOX10-positive cells in both primary and metastatic tumors (41), the frequent tumor retention of wild-type SOX10 protein and the effect of reduced SOX10 levels on RB and E2F1 levels, leading to decreased cell-cycle progression and melanoma cell proliferation, SOX10 is revealed as a notable molecule for further assessment as a therapeutic target.

Disclosure of Potential Conflicts of Interest

No potential conflicts of interest were disclosed.

Authors' Contributions

Conception and design: J.C. Cronin, D.E. Watkins-Chow, R. Dummer, S.K. Loftus, W.J. Pavan

Development of methodology: J.C. Cronin, A. Incao, S.K. Loftus

Acquisition of data (provided animals, acquired and managed patients, provided facilities, etc.): J.C. Cronin, A. Incao, J.H. Hasskamp, N. Schönewolf, L. G. Aoude, N.K. Hayward, B.C. Bastian, S.K. Loftus, W.J. Pavan

Analysis and interpretation of data (e.g., statistical analysis, biostatistics, computational analysis): J.C. Cronin, D.E. Watkins-Chow, L.G. Aoude, R. Dummer, S.K. Loftus, W.J. Pavan

Writing, review, and/or revision of the manuscript: J.C. Cronin, D.E. Watkins-Chow, J.H. Hasskamp, N.K. Hayward, B.C. Bastian, R. Dummer, S.K. Loftus, W.J. Pavan

Administrative, technical, or material support (i.e., reporting or organizing data, constructing databases): N. Schönewolf

Study supervision: W.J. Pavan

Acknowledgments

The authors thank Anand K. Ganesan for generously providing pLKO1 shRNA and lentiviral packaging plasmid, Laura L. Baxter and Ashani T. Weeraratna for manuscript assistance, Amy M. Avergas and John L. Zapas for communications regarding cell lines acquired from the Maryland Melanoma Center at Medstar Franklin Square Medical Center, and Ken Dutton-Regester for assistance with cell culture and DNA extraction.

Grant Support

This work was supported by the National Human Genome Research Institute, NIH, and the National Health and Medical Research Council of Australia (NHMRC). N.K. Hayward is supported by a Senior Principal Research Fellowship from the NHMRC.

The costs of publication of this article were defrayed in part by the payment of page charges. This article must therefore be hereby marked *advertisement* in accordance with 18 U.S.C. Section 1734 solely to indicate this fact.

Received December 18, 2012; revised July 11, 2013; accepted July 24, 2013; published OnlineFirst August 1, 2013.

References

1. Siegel R, Naishadham D, Jemal A. Cancer statistics, 2013. CA Cancer J Clin 2013;63:11–30.
2. Broekaert SMC, Roy R, Okamoto I, van den Oord J, Bauer J, Garbe C, et al. Genetic and morphologic features for melanoma classification. Pigment Cell Melanoma Res 2010;23:763–70.
3. Whiteman DC, Pavan WJ, Bastian BC. The melanomas: a synthesis of epidemiological, clinical, histopathological, genetic, and biological aspects, supporting distinct subtypes, causal pathways, and cells of origin. Pigment Cell Melanoma Res 2011;24:879–97.
4. Krauthammer M, Kong Y, Ha BH, Evans P, Bacchiocchi A, McCusker JP, et al. Exome sequencing identifies recurrent somatic RAC1 mutations in melanoma. Nat Genet 2012;44:1006–14.
5. Hodis E, Watson IR, Kryukov GV, Arold ST, Imielinski M, Theurillat J-P, et al. A landscape of driver mutations in melanoma. Cell 2012;150:251–63.
6. Pérez-Lorenzo R, Zheng B. Targeted inhibition of BRAF kinase: opportunities and challenges for therapeutics in melanoma. Biosci Rep 2012;32:25–33.

7. Narita M, Nuñez S, Heard E, Narita M, Lin AW, Hearn SA, et al. Rb-mediated heterochromatin formation and silencing of E2F target genes during cellular senescence. Cell 2003;113:703–16.
8. Chaoui A, Watanabe Y, Touraine R, Baral V, Goossens M, Pingault V, et al. Identification and functional analysis of SOX10 missense mutations in different subtypes of Waardenburg syndrome. Hum Mutat 2011;32:1436–49.
9. Garraway LA, Widlund HR, Rubin MA, Getz G, Berger AJ, Ramaswamy S, et al. Integrative genomic analyses identify MITF as a lineage survival oncogene amplified in malignant melanoma. Nature 2005;436:117–22.
10. Cronin JC, Wunderlich J, Loftus SK, Prickett TD, Wei X, Ridd K, et al. Frequent mutations in the MITF pathway in melanoma. Pigment Cell Melanoma Res 2009;22:435–44.
11. McGill GG, Horstmann M, Widlund HR, Du J, Motyckova G, Nishimura EK, et al. Bcl2 regulation by the melanocyte master regulator Mitf modulates lineage survival and melanoma cell viability. Cell 2002; 109:707–18.
12. Cheli Y, Giuliano S, Guiliano S, Botton T, Rocchi S, Hofman V, et al. Mitf is the key molecular switch between mouse or human melanoma initiating cells and their differentiated progeny. Oncogene 2011;30: 2307–18.
13. Giuliano S, Cheli Y, Ohanna M, Bonet C, Beuret L, Bille K, et al. Microphthalmia-associated transcription factor controls the DNA damage response and a lineage-specific senescence program in melanomas. Cancer Res 2010;70:3813–22.
14. Loercher AE, Tank EMH, Delston RB, Harbour JW. MITF links differentiation with cell cycle arrest in melanocytes by transcriptional activation of INK4A. J Cell Biol 2005;168:35–40.
15. Trent JM, Stanbridge EJ, McBride HL, Meese EU, Casey G, Araujo DE, et al. Tumorigenicity in human melanoma cell lines controlled by introduction of human chromosome 6. Science 1990;247:568–71.
16. Sharma BK, Manglik V, O'Connell M, Weeraratna A, McCarron EC, Broussard JN, et al. Clonal dominance of CD133+ subset population as risk factor in tumor progression and disease recurrence of human cutaneous melanoma. Int J Oncol 2012;41:1570–6.
17. Root DE, Hacohen N, Hahn WC, Lander ES, Sabatini DM. Genome-scale loss-of-function screening with a lentiviral RNAi library. Nat Methods 2006;3:715–9.
18. Narla G, Difeo A, Reeves HL, Schaid DJ, Hirshfeld J, Hod E, et al. A germline DNA polymorphism enhances alternative splicing of the KLF6 tumor suppressor gene and is associated with increased prostate cancer risk. Cancer Res 2005;65:1213–22.
19. Jang YK, Park JJ, Lee MC, Yoon BH, Yang YS, Yang SE, et al. Retinoic acid-mediated induction of neurons and glial cells from human umbilical cord-derived hematopoietic stem cells. J Neurosci Res 2004;75: 573–84.
20. Pollock PM, Cohen-Solal K, Sood R, Namkoong J, Martino JJ, Koganti A, et al. Melanoma mouse model implicates metabotropic glutamate signaling in melanocytic neoplasia. Nat Genet 2003;34:108–12.
21. Britsch S, Goerich DE, Riethmacher D, Peirano RI, Rossner M, Nave KA, et al. The transcription factor Sox10 is a key regulator of peripheral glial development. Genes Dev 2001;15:66–78.
22. Hodgkinson CA, Moore KJ, Nakayama A, Steingrímsson E, Copeland NG, Jenkins NA, et al. Mutations at the mouse microphthalmia locus are associated with defects in a gene encoding a novel basic-helix-loop-helix-zipper protein. Cell 1993;74:395–404.
23. Bernex F, De Sepulveda P, Kress C, Elbaz C, Delouis C, Panthier JJ. Spatial and temporal patterns of c-kit-expressing cells in WlacZ/+ and WlacZ/WlacZ mouse embryos. Development 1996;122:3023–33.
24. Matera I, Watkins-Chow DE, Loftus SK, Hou L, Incao A, Silver DL, et al. A sensitized mutagenesis screen identifies Gli3 as a modifier of Sox10 neurocristopathy. Hum Mol Genet 2008;17:2118–31.
25. Houghton AN, Real FX, Davis LJ, Cordon-Cardo C, Old LJ. Phenotypic heterogeneity of melanoma. Relation to the differentiation program of melanoma cells. J Exp Med 1987;164:812–29.
26. Halaban R. Rb/E2F: a two-edged sword in the melanocytic system. Cancer Metastasis Rev 2005;24:339–56.
27. Li CG, Nyman JE, Braithwaite AW, Eccles MR. PAX8 promotes tumor cell growth by transcriptionally regulating E2F1 and stabilizing RB protein. Oncogene 2011;30:4824–34.
28. Fenouille N, Robert G, Tichet M, Puissant A, Dufies M, Rocchi S, et al. The p53/p21Cip1/Waf1 pathway mediates the effects of SPARC on melanoma cell cycle progression. Pigment Cell Melanoma Res 2011;24:219–32.
29. Carreira S, Goodall J, Denat L, Rodriguez M, Nuciforo P, Hoek KS, et al. Mitf regulation of Dia1 controls melanoma proliferation and invasiveness. Genes Dev 2006;20:3426–39.
30. Potterf SB, Furumura M, Dunn KJ, Arnheiter H, Pavan WJ. Transcription factor hierarchy in Waardenburg syndrome: regulation of MITF expression by SOX10 and PAX3. Hum Genet 2000;107:1–6.
31. Du J, Widlund HR, Horstmann MA, Ramaswamy S, Ross K, Huber WE, et al. Critical role of CDK2 for melanoma growth linked to its melanocyte-specific transcriptional regulation by MITF. Cancer Cell 2004;6:565–76.
32. Carreira S, Goodall J, Aksan I, La Rocca SA, Galibert M-D, Denat L, et al. Mitf cooperates with Rb1 and activates p21Cip1 expression to regulate cell cycle progression. Nature 2005;433:764–9.
33. Liu F, Singh A, Yang Z, Garcia A, Kong Y, Meyskens FL. MiTF links Erk1/2 kinase and p21CIP1/WAF1 activation after UVC radiation in normal human melanocytes and melanoma cells. Mol Cancer 2010; 9:214.
34. Prickett TD, Wei X, Cardenas-Navia I, Teer JK, Lin JC, Walia V, et al. Exon capture analysis of G protein-coupled receptors identifies activating mutations in GRM3 in melanoma. Nat Genet 2011;43:1119–26.
35. Wei X, Walia V, Lin JC, Teer JK, Prickett TD, Gartner J, et al. Exome sequencing identifies GRIN2A as frequently mutated in melanoma. Nat Genet 2011;43:442–6.
36. Hornyak TJ, Jiang S, Guzmán EA, Scissors BN, Tuchinda C, He H, et al. Mitf dosage as a primary determinant of melanocyte survival after ultraviolet irradiation. Pigment Cell Melanoma Res 2009;22:307–18.
37. Paraiso KHT, Xiang Y, Rebecca VW, Abel EV, Chen YA, Munko AC, et al. PTEN loss confers BRAF inhibitor resistance to melanoma cells through the suppression of BIM expression. Cancer Res 2011;71: 2750–60.
38. Alcala AM, Flaherty KT. BRAF inhibitors for the treatment of metastatic melanoma: clinical trials and mechanisms of resistance. Clin Cancer Res 2012;18:33–9.
39. Nonaka D, Chiriboga L, Rubin BP. Sox10: a pan-schwannian and melanocytic marker. Am J Surg Pathol 2008;32:1291–8.
40. Bakos RM, Maier T, Besch R, Mestel DS, Ruzicka T, Sturm RA, et al. Nestin and SOX9 and SOX10 transcription factors are coexpressed in melanoma. Exp Dermatol 2010;19:e89–94.
41. Agnarsdóttir M, Sooman L, Bolander A, Strömberg S, Rexhepaj E, Bergqvist M, et al. SOX10 expression in superficial spreading and nodular malignant melanomas. Melanoma Res 2010;20:468–78.
42. Flammiger A, Besch R, Cook AL, Maier T, Sturm RA, Berking C. SOX9 and SOX10 but Not BRN2 are required for nestin expression in human melanoma cells. J Invest Dermatol 2008;129:945–53.
43. Berger MF, Hodis E, Heffernan TP, Deribe YL, Lawrence MS, Protopopov A, et al. Melanoma genome sequencing reveals frequent PREX2 mutations. Nature 2012;485:502–6.
44. Hofmann F, Martelli F, Livingston DM, Wang Z. The retinoblastoma gene product protects E2F-1 from degradation by the ubiquitin-proteasome pathway. Genes Dev 1996;10:2949–59.
45. Boyer SN, Wazer DE, Band V. E7 protein of human papilloma virus-16 induces degradation of retinoblastoma protein through the ubiquitin-proteasome pathway. Cancer Res 1996;56:4620–4.
46. Jiang X, Zhou J, Giobbie-Hurder A, Wargo J, Hodi FS. The activation of MAPK in melanoma cells resistant to BRAF inhibition promotes PD-L1 expression that is reversible by MEK and PI3K inhibition. Clin Cancer Res 2013;19:598–609.
47. Shakhova O, Zingg D, Schaefer SM, Hari L, Civenni G, Blunschi J, et al. Sox10 promotes the formation and maintenance of giant congenital naevi and melanoma. Nat Cell Biol 2012;14:882–90.